Analytical study of coherence in seeded modulation instability

J. Bonetti and S. M. Hernandez
Instituto Balseiro, Avenida Bustillo km 9.500, Bariloche R8402AGP, Argentina

P. I. Fierens
Instituto Tecnológico de Buenos Aires, Eduardo Madero 399, Buenos Aires C1106ACD, Argentina
and Consejo Nacional de Investigaciones Científicas y Técnicas (CONICET), Argentina

D. F. Grosz
Instituto Balseiro, Avenida Bustillo km 9.500, Bariloche R8402AGP, Argentina
and Consejo Nacional de Investigaciones Científicas y Téecnicas (CONICET), Argentina
(Received 12 June 2016; published 15 September 2016)

We derive analytical expressions for the coherence in the onset of modulation instability, in excellent agreement with thorough numerical simulations. As usual, we start by a linear perturbation analysis, where broadband noise is added to a cw pump; then, we investigate the effect of adding a deterministic seed to the cw pump, a case of singular interest as it is commonly encountered in parametric amplification schemes. Results for the dependence of coherence on parameters such as fiber type, pump power, propagated distance, and seed signal-to-noise ratio are presented. Finally, we show the importance of including higher-order linear and nonlinear dispersion when looking at longer-wavelength regions (mid IR).

DOI: 10.1103/PhysRevA.94.033826

I. INTRODUCTION

In this work, we study analytically the problem of modulation instability in optical fibers with noisy inputs. In particular, we focus on the phase coherence of the resulting spectrum. One metric of phase coherence is given by [1,2]

$$g_{12}(z,\Omega) = \frac{\langle \tilde{a}_k^*(z,\Omega)\tilde{a}_l(z,\Omega)\rangle_{k\neq l}}{\sqrt{\langle|\tilde{a}_k(z,\Omega)|^2\rangle\langle|\tilde{a}_l(z,\Omega)|^2\rangle}}, \tag{1}$$

where $\tilde{a}(z,\Omega)$ is the Fourier transform of the pulse envelope at position z along the fiber, Ω is the frequency, the subscripts k and l correspond to different realizations, and the angle brackets denote ensemble averages. This metric is widely used in the area of supercontinuum (SC) generation (see, e.g., [3,4] and references therein). The relation between modulation instability (MI) and SC has been a matter of profound analysis (see, for example, [5,6]). Moreover, modulation instability, being seeded by the noise at the input, is one of the sources of fluctuations in cw-generated supercontinuum spectra. We must note that the relation of the pump noise to supercontinuum generation has been widely studied (see, e.g., [7–14] and references therein).

There also have been other attempts at dealing analytically with MI and noisy inputs. For example, Aslam *et al.* [15] study the problem, but they do not include either higher-order dispersion or Raman scattering. Our development, in contrast, follows the same path as the usual modulation instability analysis, i.e., we investigate a perturbation to a continuous wave, including all relevant terms of the generalized nonlinear Schrödinger equation that models propagation in optical fibers.

In Sec. II, we develop analytical expressions for g_{12} when the input is a noisy perturbation to a continuous wave. Specifically, the input perturbation spectrum is given by $\tilde{a}(0,\Omega) = \tilde{s}(\Omega) + \tilde{N}(\Omega)$, where $\tilde{s}(\Omega)$ is the Fourier transform of the deterministic seed and $\tilde{N}(\Omega)$ corresponds to additive white Gaussian noise. Such noise may be considered as an approximation to the shot noise typical of a laser output. Since expressions are somewhat complex, we provide examples of their use for some particular inputs and limiting cases. In Sec. II A, we specialize the equations to the case in which $\tilde{s}(\Omega) = 0$ for $\Omega < 0$. This situation corresponds to the very important case of a seed wavelength alongside with the pump. Section II B presents results corresponding to the case of a symmetrical power spectrum, i.e., $|\tilde{s}(\Omega)| = |\tilde{s}(-\Omega)|$. Finally, Sec. II C deals with the case where there is only noise at the input of the optical fiber, that is, $\tilde{s}(\Omega) = 0$. Since coherence, as defined in Eq. (1), is not particularly enlightening in this case, we study other metrics that provide some information on the MI spectrum.

A comparison of the analytical results with simulations is presented in Sec. III. Final conclusions are presented in Sec. IV.

II. BROADBAND NOISE AS A PERTURBATION TO A CW PUMP

Wave propagation in lossless optical fibers can be described by the generalized nonlinear Schrödinger equation [16]:

$$\frac{\partial A}{\partial z} - i\hat{\beta}A = i\hat{\gamma}A(z,T)\int_{-\infty}^{+\infty} R(T')|A(z,T-T')|^2 dT', \tag{2}$$

where $A(z,T)$ is the slowly varying envelope, z is the spatial coordinate, and T is the time coordinate in a comoving frame at the group velocity ($= \beta_1^{-1}$). $\hat{\beta}$ and $\hat{\gamma}$ are operators related to the dispersion and nonlinearity, respectively, and are defined by

$$\hat{\beta} = \sum_{m\geqslant 2} \frac{i^m}{m!}\beta_m \frac{\partial^m}{\partial T^m}, \quad \hat{\gamma} = \sum_{n\geqslant 0} \frac{i^n}{n!}\gamma_n \frac{\partial^n}{\partial T^n}.$$

The β_m's are the coefficients of the Taylor expansion of the propagation constant $\beta(\omega)$ about a central frequency ω_0. In

the convolution integral in the right-hand side of Eq. (2), $R(T)$ is the nonlinear-response function including both the instantaneous (electronic) and delayed Raman response.

Modulation instability is customarily analyzed by studying the evolution of a small perturbation a to the stationary solution of Eq. (2):

$$A(z,T) = (\sqrt{P_0} + a(z,T))e^{i\gamma_0 P_0 z}. \tag{3}$$

By only keeping terms linear in the perturbation, after some straightforward algebra, substitution of Eq. (3) into Eq. (2) leads to the following second-order ordinary differential equation in the frequency domain:

$$\frac{\partial^2 \tilde{a}(z,\Omega)}{\partial z^2} + 2i\tilde{B}(\Omega)\frac{\partial \tilde{a}(z,\Omega)}{\partial z} - \tilde{C}(\Omega)\tilde{a}(z,\Omega) = 0, \tag{4}$$

where $\Omega = \omega - \omega_0$, and $\tilde{a}$ and $\tilde{R}$ are the Fourier transforms of a and R, respectively, where, for the sake of clarity, we have introduced the variables

$$\begin{aligned}
\tilde{B}(\Omega) &= -[\tilde{\beta}_o(\Omega) + P_0\tilde{\gamma}_o(\Omega)(1+\tilde{R}(\Omega))],\\
\tilde{C}(\Omega) &= \tilde{\beta}_o^2(\Omega) - \tilde{\beta}_e^2(\Omega) + P_0^2\big(\tilde{\gamma}_o^2(\Omega) - \tilde{\gamma}_e^2(\Omega)\big)(1+2\tilde{R}(\Omega))\\
&\quad - P_0^2\gamma_0^2 + 2P_0\gamma_0\tilde{\beta}_e(\Omega) + 2P_0^2\gamma_0\tilde{\gamma}_e(\Omega)(1+\tilde{R}(\Omega))\\
&\quad + 2P_0(\tilde{\beta}_o\tilde{\gamma}_o - \tilde{\beta}_e\tilde{\gamma}_e)(1+\tilde{R}(\Omega)),\\
\tilde{\beta}_e(\Omega) &= \sum_{n\geqslant 1}\frac{\beta_{2n}}{(2n)!}\Omega^{2n}, \quad \hat{\beta}_o(\Omega) = \sum_{n\geqslant 1}\frac{\beta_{2n+1}}{(2n+1)!}\Omega^{2n+1},\\
\tilde{\gamma}_e(\Omega) &= \sum_{n\geqslant 0}\frac{\gamma_{2n}}{(2n)!}\Omega^{2n}, \quad \hat{\gamma}_o(\Omega) = \sum_{n\geqslant 0}\frac{\gamma_{2n+1}}{(2n+1)!}\Omega^{2n+1}.
\end{aligned}$$

Substitution of the ansatz $a(z,\Omega) = D\exp[iK(\Omega)z]$ in Eq. (4) leads to

$$K^2(\Omega) + 2K(\Omega)\tilde{B}(\Omega) + \tilde{C}(\Omega) = 0.$$

Finally, the dispersion relation obtained as a solution to this equation is

$$K(\Omega) = -\tilde{B}(\Omega) \pm \sqrt{\tilde{B}^2(\Omega) - \tilde{C}(\Omega)}. \tag{5}$$

This expression agrees with those found in the literature (see, e.g., [17]). As usual, MI gain can be found as the imaginary part of $K(\Omega)$.

Some further calculations show that the spectral evolution of the perturbation can be written as

$$\tilde{a}(z,\Omega) = \frac{e^{-i\tilde{B}(\Omega)z}}{K_D(\Omega)}[D_z(\Omega)\tilde{a}^*(0,-\Omega) + F_z(\Omega)\tilde{a}(0,\Omega)], \tag{6}$$

where $K_D(\Omega) = \sqrt{\tilde{B}^2(\Omega) - \tilde{C}(\Omega)}$ and

$$\begin{aligned}
D_z(\Omega) &= iP_0\tilde{\gamma}(\Omega)\tilde{R}(\Omega)\sin(K_D(\Omega)z),\\
F_z(\Omega) &= i(\tilde{\beta}_e + P_0\tilde{\gamma}_e(1+\tilde{R}) - P_0\gamma_0)\sin(K_D z)\\
&\quad + K_D\cos(K_D z).
\end{aligned}$$

Let us assume that $a(0,\Omega) = \tilde{s}(\Omega) + \tilde{N}(\Omega)$, where $\tilde{s}(\Omega)$ is the Fourier transform of a deterministic seed and $\tilde{N}(\Omega)$ are independent and identically distributed circularly symmetric normal variables with variance σ^2 for each Ω, i.e., $\tilde{N}(\Omega) \sim \mathcal{CN}(0,\sigma^2)$. If $a_k(z,\Omega)$, $k \in \mathbb{N}$, are independent realizations, then, by Eq. (6)

$$\begin{aligned}
&\langle \tilde{a}_k^*(z,\Omega)\tilde{a}_l(z,\Omega)\rangle\\
&\quad = \left|\frac{e^{-i\tilde{B}(\Omega)z}}{K_D(\Omega)}\right|^2\{|D_z(\Omega)|^2|\tilde{s}(-\Omega)|^2 + |F_z(\Omega)|^2|\tilde{s}(\Omega)|^2\\
&\qquad + 2\mathrm{Re}\{D_z(\Omega)F_z^*(\Omega)\tilde{s}(\Omega)\tilde{s}(-\Omega)\}\},
\end{aligned} \tag{7}$$

for $k \neq l$. In the case $k = l$,

$$\begin{aligned}
&\big\langle\big|\tilde{a}_k^2(z,\Omega)\big|^2\big\rangle\\
&\quad = \left|\frac{e^{-i\tilde{B}(\Omega)z}}{K_D(\Omega)}\right|^2\{|D_z(\Omega)|^2(|\tilde{s}(-\Omega)|^2 + \sigma^2) + |F_z(\Omega)|^2\\
&\qquad \times(|\tilde{s}(\Omega)|^2 + \sigma^2) + 2\mathrm{Re}\{D_z(\Omega)F_z^*(\Omega)\tilde{s}(\Omega)\tilde{s}(-\Omega)\}\}.
\end{aligned} \tag{8}$$

Using Eqs. (7) and (8), the coherence of the perturbation becomes

$$\begin{aligned}
\frac{1}{g_{12}(z,\Omega)} &= 1 + (|D_z(\Omega)|^2 + |F_z(\Omega)|^2)\sigma^2\\
&\quad \times\{|D_z(\Omega)|^2|\tilde{s}(-\Omega)|^2 + |F_z(\Omega)|^2|\tilde{s}(\Omega)|^2\\
&\quad + 2\mathrm{Re}\{D_z(\Omega)F_z^*(\Omega)\tilde{s}(\Omega)\tilde{s}(-\Omega)\}\}^{-1}.
\end{aligned} \tag{9}$$

Finally, by a straightforward calculation g_{12} is found to depend only on the even terms β_{2k} of the expansion of the propagation constant.

A. Single sideband

As a relevant example of the use of this equation, consider the case in which, for a given Ω, $\tilde{s}(-\Omega) = 0$ and $\tilde{s}(\Omega) \neq 0$ (e.g., $\tilde{s}(\Omega) = 0$ for $\Omega < 0$). This case is of particular interest because besides the pump there is a smaller seed signal at a given wavelength, a situation commonly found in various parametric amplification schemes. Then,

$$\frac{1}{g_{12}(z,\Omega)} = 1 + \left[1 + \left(\frac{|D_z(\Omega)|^2}{|F_z(\Omega)|^2}\right)^{\mathrm{sgn}(\Omega)}\right]\frac{\sigma^2}{|\tilde{s}(|\Omega|)|^2}, \tag{10}$$

where $\mathrm{sgn}(\cdot)$ denotes the sign function. When $|\tilde{s}(|\Omega|)|^2 \gg \sigma^2$,

$$g_{12}(z,\Omega) \approx 1 - \left[1 + \left(\frac{|D_z(\Omega)|^2}{|F_z(\Omega)|^2}\right)^{\mathrm{sgn}(\Omega)}\right]\frac{\sigma^2}{|\tilde{s}(|\Omega|)|^2}.$$

It may be easier to understand these expressions in the particular case where $\gamma_n = 0$ for $n \geqslant 1$ (e.g., neglecting the effect of self-steepening) and considering only the electronic instantaneous response $[R(T) = \delta(T)]$. If we further assume that there exists MI gain,

$$\begin{aligned}
&\frac{1}{g_{12}(z,\Omega)}\\
&\quad = 1 + \left[1 + \left(\frac{\gamma_0^2P_0^2\sinh^2(g(\Omega)z/2)}{\gamma_0^2P_0^2\sinh^2(g(\Omega)z/2) + \frac{1}{4}g^2(\Omega)}\right)^{\mathrm{sgn}(\Omega)}\right]\\
&\qquad \times\frac{\sigma^2}{|\tilde{s}(|\Omega|)|^2},
\end{aligned}$$

where $g(\Omega) = 2K_D(\Omega)/i$ is the modulation gain. Interesting expressions are obtained in two limiting cases, when either

$g(\Omega)z \ll 1$ (propagated distance much shorter than the MI length) or $g(\Omega)z \gg 1$ (propagated distance much longer than the MI length). In the former case,

$$\gamma_0^2 P_0^2 \sinh^2(g(\Omega)z/2) \approx \gamma_0^2 P_0^2 (g(\Omega)z/2)^2 \approx \frac{g^2(\Omega)}{4}\left(\frac{z}{L_{\rm NL}}\right)^2,$$

whereas $L_{\rm NL} = (\gamma_0 P_0)^{-1}$ is the usual nonlinear length. Thus,

$$g_{12}(z,\Omega) \approx 1 - \left\{1 + \left[1 + \left(\frac{L_{\rm NL}}{z}\right)^2\right]^{-{\rm sgn}(\Omega)}\right\} \frac{\sigma^2}{|\tilde{s}(|\Omega|)|^2}.$$

Note that coherence does not depend on the actual MI gain. If we further assume that $z \ll L_{\rm NL}$,

$$g_{12}(z,\Omega) \approx \begin{cases} 1 - \left[1 + \left(\frac{z}{L_{\rm NL}}\right)^2\right] \frac{\sigma^2}{|\tilde{s}(|\Omega|)|^2} & \Omega > 0, \\ 1 - \left[2 + \left(\frac{L_{\rm NL}}{z}\right)^2\right] \frac{\sigma^2}{|\tilde{s}(|\Omega|)|^2} & \Omega < 0. \end{cases}$$

It is clear from this equation that, while coherence decreases as z increases for $\Omega > 0$, it increases with z for $\Omega < 0$.

In the case where $g(\Omega)z \gg 1$, coherence depends neither on the particular MI gain nor on the sign of Ω, and

$$g_{12}(z,\Omega) \approx 1 - 2\frac{\sigma^2}{|\tilde{s}(|\Omega|)|^2}. \tag{11}$$

In this respect, as z increases, coherences of Stokes and anti-Stokes components approach the same value.

B. Equal power spectrum sidebands

Another particular case is when $|\tilde{s}(-\Omega)| = |\tilde{s}(\Omega)|$. This case corresponds to that where the pump is modulated by two smaller signals of the same amplitude, located symmetrical to the pump (in the frequency space.) In this case,

$$\frac{1}{g_{12}(z,\Omega)} = 1 + \frac{1}{1 + \frac{2{\rm Re}\{D_z(\Omega)F_z^*(\Omega)e^{i(\phi_s(\Omega)+\phi_s(-\Omega))}\}}{|D_z(\Omega)|^2+|F_z(\Omega)|^2}} \frac{\sigma^2}{|\tilde{s}(\Omega)|^2},$$

where $\phi_s(\Omega) = \arg\{\tilde{s}(\Omega)\}$. It is interesting to note that coherence depends on the phase relation: $\phi_s(\Omega) + \phi_s(-\Omega)$. In particular, coherence is maximized when

$${\rm Re}\{D_z(\Omega)F_z^*(\Omega)e^{i(\phi_s(\Omega)+\phi_s(-\Omega))}\} = |D_z(\Omega)||F_z(\Omega)|.$$

So, we can write that

$$\frac{1}{g_{12}(z,\Omega)} \geqslant 1 + \frac{1}{1 + \frac{2|D_z(\Omega)||F_z(\Omega)|}{|D_z(\Omega)|^2+|F_z(\Omega)|^2}} \frac{\sigma^2}{|\tilde{s}(\Omega)|^2}.$$

From this expression, it is simple to prove that

$$g_{12}(z,\Omega) \leqslant \frac{1}{1 + \frac{1}{2}\frac{\sigma^2}{|\tilde{s}(\Omega)|^2}} \approx 1 - \frac{1}{2}\frac{\sigma^2}{|\tilde{s}(\Omega)|^2}, \tag{12}$$

where the approximation is valid for large input signal-to-noise ratio.

It is interesting to compare Eqs. (11) and (12). It might be argued that the double-sideband case may lead to a higher spectral coherence than the single-sideband one. However, it must be noted that the higher coherence can be achieved by tuning the phase of the input seed. In the particular case of two input pulses at frequencies symmetrical with respect to the pump, only a particular phase relationship maximizes coherence.

C. Noise as input

We now turn our attention to the case where $a(0,\Omega) = \tilde{N}(\Omega)$, with i.i.d. $\tilde{N}(\Omega) \sim \mathcal{CN}(0,\sigma^2)$. Equation (9) implies that coherence is zero in this case. However, there are other characteristics of the MI spectrum that can be analytically calculated.

From Eq. (6), it follows that $\tilde{a}(z,\Omega)$ is also a circularly symmetric normal random variable. Moreover, its variance is given by

$$\sigma_{\tilde{a}}^2 = \sigma^2 \left|\frac{e^{-i\tilde{B}(\Omega)z}}{K_D(\Omega)}\right|^2 \{|\tilde{M}(\Omega)\sin(K_D(\Omega)z)|^2 + |K_D(\Omega)\cos(K_D(\Omega)z) - (\tilde{N}(\Omega) - i\tilde{B}(\Omega))\sin(K_D(\Omega)z)|^2\}. \tag{13}$$

Higher moments of the power spectrum are sometimes of interest [18]. Since $\tilde{a}(z,\Omega)$ is circularly symmetric, $|\tilde{a}(z,\Omega)|$ has a Rayleigh distribution with scale parameter $\sigma_{\tilde{a}}$ [i.e., with a probability density function $f(x;\sigma_{\tilde{a}}) = \frac{x}{\sigma_{\tilde{a}}^2} e^{-x^2/(2\sigma_{\tilde{a}}^2)}$, $x \geqslant 0$] and $|\tilde{a}(z,\Omega)|^2/\sigma_{\tilde{a}}^2$ has a χ^2 distribution with two degrees of freedom. By straight calculation we obtain

$$\text{skewness}\,(|\tilde{a}(z,\Omega)|^2) = 2, \tag{14}$$

$$\text{excess kurtosis}\,(|\tilde{a}(z,\Omega)|^2) = 6. \tag{15}$$

It is also interesting to note that the χ^2 distribution has a long right tail (as evidenced, for example, by the excess kurtosis.) This fact implies a non-negligible probability of high power spectral densities.

Another interesting metric is the signal-to-noise ratio. The definition given by Sørensen *et al.* [18,19] in the context of a

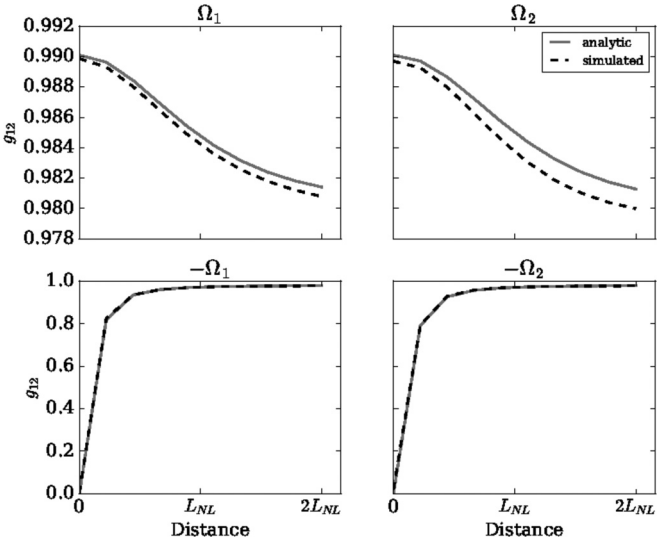

FIG. 1. $g_{12}(\Omega)$ vs distance. Analytical (full line) and numerical (dashed line) results. Seed frequencies are $\Omega = \pm\Omega_{1,2}$ for $\Omega_1 = 31$ GHz and $\Omega_2 = 46$ GHz. Fiber type is SSMF.

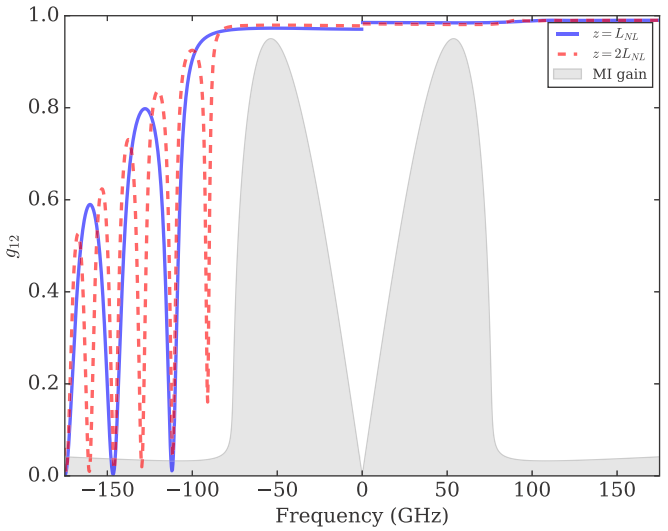

FIG. 2. $g_{12}(\Omega)$ vs frequency at distances L_{NL} and $2L_{\mathrm{NL}}$, and for a SSMF fiber ($P_0 = 1$ W).

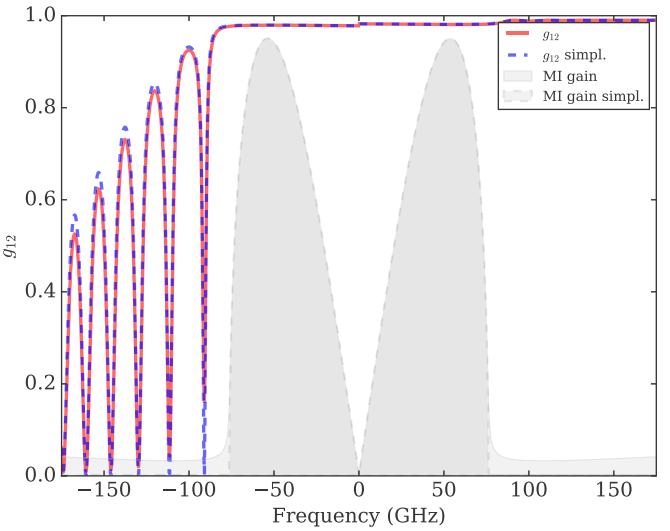

FIG. 4. $g_{12}(\Omega)$ at distance $2L_{\mathrm{NL}}$ for a simplified fiber ($\beta_{n\geqslant 3} = 0$, no self-steepening, and no Raman) vs complete fiber model.

supercontinuum is

$$\mathrm{SNR}(\Omega) = \frac{\langle|\tilde{a}(z,\Omega)|^2\rangle}{\sqrt{\mathrm{Var}(|\tilde{a}(z,\Omega)|^2)}}, \tag{16}$$

where $\mathrm{Var}(X) = \langle|X - \langle X\rangle|^2\rangle$. It is easy to see that, in our case, $\mathrm{SNR}(\Omega) = 1$ for all Ω.

III. RESULTS

In order to test the validity of our analytical results, in Fig. 1 we compare the value of g_{12} by seeding with 1 mW power at frequencies 31 and 46 GHz, and show its evolution along a standard single-mode fiber [SSMF, $\beta_2 = -21\,\mathrm{ps}^2/\mathrm{km}$, $\beta_3 = 0.184\,\mathrm{ps}^3/\mathrm{km}$, and $\gamma_0 = 1.2\,(\mathrm{W\,km})^{-1}$] over a distance of $2L_{\mathrm{NL}}$ for both the Stokes and anti-Stokes sidebands, and for a pump power of 1 W at 1550 nm (corresponding to 193.4 THz). The nonlinear response $R(T)$ is that of silica fibers and the self-steepening term γ_1 is calculated as γ_0/ω_0 [16]. It can be seen that the analytically evaluated g_{12} [Eq. (10)] is in excellent agreement with the one calculated from 300 noise realizations (a total of 150×299 averaged correlations), where the seed signal-to-noise ratio is 10 dB. Also, the "same limit" property stated in Eq. (11) is verified.

In Figs. 2 and 3, we depict $g_{12}(\Omega)$ when seeding with 1 mW power at frequencies $\Omega > 0$, 10 dB input signal-to-noise ratio, and for distances L_{NL} and $2L_{\mathrm{NL}}$. While in Fig. 2 we show results for a SSMF fiber, in Fig. 3, for comparison, results shown correspond to a nonzero dispersion-shifted fiber (NZ-DSF, same β_2 as SSMF, $\beta_3 = 0.108\,\mathrm{ps}^3/\mathrm{km}$, $\gamma_0 = 1.6\,(\mathrm{W\,km})^{-1}$). By looking at the lower frequency side of the spectrum, we see that coherence (i.e., the value of g_{12}) increases with distance up to the limit given by Eq. (11), as expected. A "coherence bandwidth," defined as the frequency range from the pump frequency to the first coherence minimum, is observed to diminish with increasing distance for both fiber types, limiting the region where high coherence components are generated.

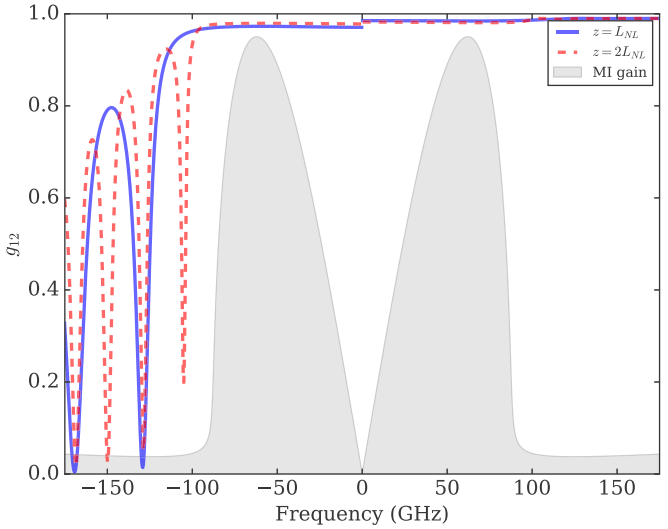

FIG. 3. $g_{12}(\Omega)$ vs frequency at distances L_{NL} and $2L_{\mathrm{NL}}$, and for a NZ DSF fiber ($P_0 = 1$ W).

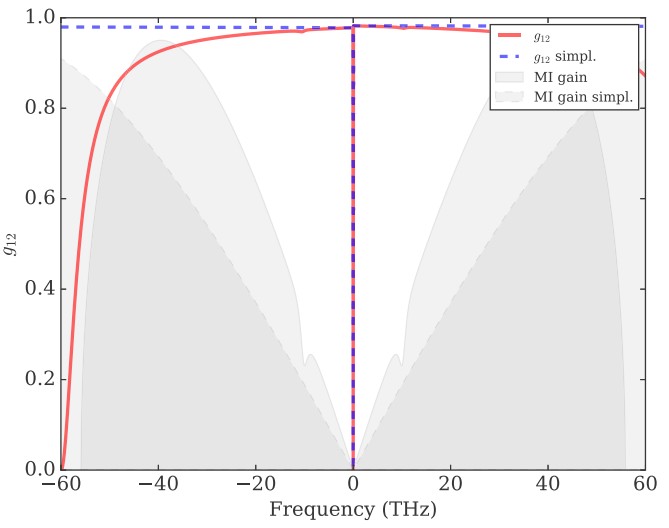

FIG. 5. Same as Fig. 4 in the mid-IR spectral region.

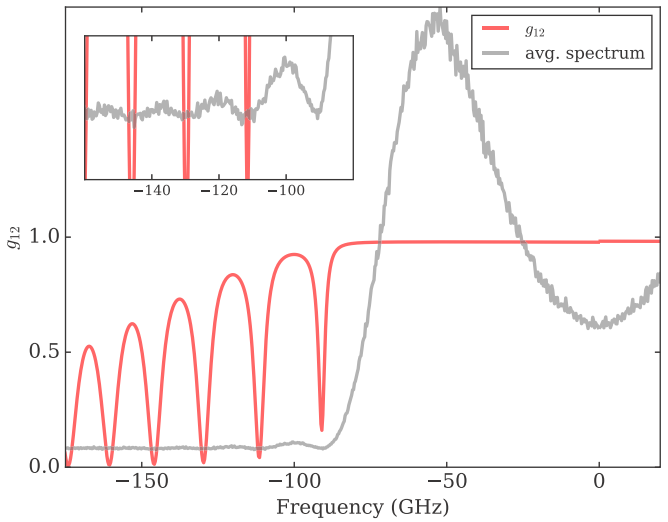

FIG. 6. g_{12} vs analytic averaged spectra. Zeroes in the coherence function follow ripples in the spectrum.

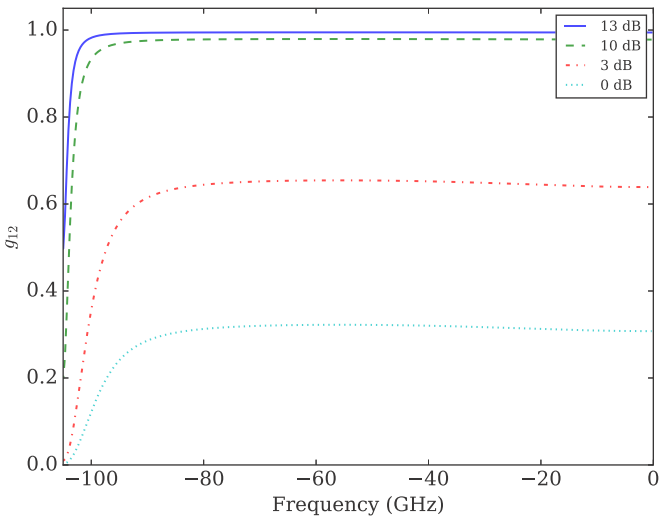

FIG. 8. g_{12} Stokes-side "coherence bandwidth" for different signal-to-noise ratios at $2L_{\mathrm{NL}}$ (NZ-DSF fiber).

The width of this region is strongly dependent on the MI gain profile (overlayed for comparison), and clearly the higher nonlinearity of the NZ-DSF yields a larger coherent bandwidth as compared to SSMF.

In both Figs. 2 and 3 a complete model that includes Raman and self-steepening is used, whereas in Fig. 4 we compare the complete model for SSMF of Figs. 1 and 2 at distance $2L_{\mathrm{NL}}$, to the simplified case where neither Raman nor self-steepening nor higher-order linear dispersion are present. The difference is nearly negligible. To show that this is not always the case, in Fig. 5 we consider the same comparison as in Fig. 4, but for a typical chalcogenide fiber (see, e.g., [20,21]) in the mid-IR spectral region, where the influence of self-steepening is greatly augmented for two reasons: chalcogenide fibers typically possess nonlinear coefficients γ_0 100 to 1000 times larger than those of silica fibers; plus, the larger wavelengths in the mid-IR range render the self-steepening term γ_1 ($\approx \gamma_0/\omega_0$) many times larger than that in the telecommunication band.

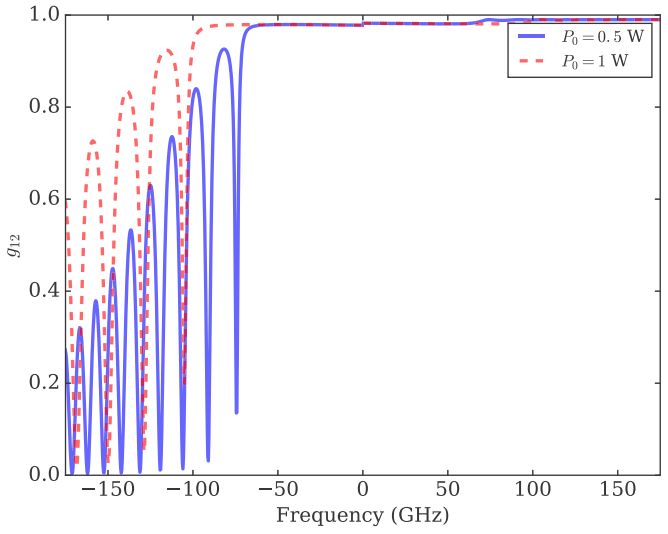

FIG. 7. g_{12} for different pump powers at $2L_{\mathrm{NL}}$ (NZ-DSF fiber).

Consequently, in this case, not considering the complete model leads to wrong results.

It is interesting to point out that, although higher coherence is tightly connected to the region where there is MI gain, the presence of decreasing lobes of considerable coherence beyond the MI cutoff frequency becomes apparent. In Fig. 6 we show $g_{12}(\Omega)$ against a scaled plot of the averaged spectra of 2000 noise realizations. A strong correlation between g_{12} side lobes and spectral ripples is evident. Also, the MI gain cutoff frequency grows with increasing power. As such, Fig. 7 shows the enlargement of the coherence bandwidth when increasing the pump power from 500 mW to 1 W.

Finally, when fixing both pump power (1 W) and distance ($2L_{\mathrm{NL}}$), varying the seed signal-to-noise power ratio has little effect on the the coherence bandwidth; however, the 3-dB point (as measured from $\Omega = 0$ to the point where the maximum g_{12} has decreased to $g_{12}/2$) grows monotonically, as it can be seen in Fig. 8.

IV. CONCLUSIONS

In this paper we derived analytical expressions for the coherence in the onset of modulation instability in excellent agreement with numerical simulations. We focused on the case where broadband noise is added to a continuous wave pump (with wavelength lying in the telecommunication near the IR band) and investigated the effect of adding a deterministic seed to the cw pump, a case of singular interest as it is commonly encountered in parametric amplification schemes. We obtained results for the dependence of coherence on parameters such as fiber type, pump power, propagated distance, and the signal-to-noise ratio of the seed wavelength. We also investigated the coherence bandwidth, finding that nonzero dispersion shifted fibers yield a greater bandwidth than standard single-mode fibers. Interestingly, in both cases, the coherence bandwidth extends beyond the MI gain cutoff frequency.

We found that inclusion of higher-order linear and nonlinear dispersion leads to very similar results to those obtained from

a simplified model in the near-IR range, but is of critical importance when looking at higher wavelengths (mid-IR range), where the influence of the self-steepening effect is greatly augmented.

Finally, we believe these results might be of significance when analyzing the onset of supercontinuum generation from cw pumps, as they shed light into the coherence of the initial evolution stage.

[1] J. M. Dudley and S. Coen, Opt. Lett. **27**, 1180 (2002).
[2] J. M. Dudley and S. Coen, IEEE J. Sel. Top. Quantum Electron. **8**, 651 (2002).
[3] J. M. Dudley, G. Genty, and S. Coen, Rev. Mod. Phys. **78**, 1135 (2006).
[4] *Supercontinuum Generation in Optical Fibers*, edited by J. M. Dudley and J. R. Taylor (Cambridge University, Cambridge, England, 2010).
[5] A. Demircan and U. Bandelow, Opt. Commun. **244**, 181 (2005).
[6] A. Demircan and U. Bandelow, Appl. Phys. B **86**, 31 (2007).
[7] K. Corwin, N. Newbury, J. Dudley, S. Coen, S. Diddams, B. Washburn, K. Weber, and R. Windeler, Appl. Phys. B **77**, 269 (2003).
[8] N. R. Newbury, B. R. Washburn, K. L. Corwin, and R. S. Windeler, Opt. Lett. **28**, 944 (2003).
[9] A. K. Abeeluck and C. Headley, Appl. Phys. Lett. **85**, 4863 (2004).
[10] F. Vanholsbeeck, S. Martin-Lopez, M. González-Herráez, and S. Coen, Opt. Express **13**, 6615 (2005).
[11] J. M. Dudley, G. Genty, and B. J. Eggleton, Opt. Express **16**, 3644 (2008).
[12] S. M. Kobtsev and S. V. Smirnov, Opt. Express **16**, 7428 (2008).
[13] D. R. Solli, C. Ropers, and B. Jalali, Phys. Rev. Lett. **101**, 233902 (2008).
[14] D. Solli, G. Herink, B. Jalali, and C. Ropers, Nature Photonics **6**, 463 (2012).
[15] M. S. Aslam, M. Y. Hamza, and N. Sarwar, AIP Adv. **2**, 022168 (2012).
[16] G. Agrawal, *Nonlinear Fiber Optics*, 5th ed., Optics and Photonics (Academic, New York, 2012).
[17] P. Béjot, B. Kibler, E. Hertz, B. Lavorel, and O. Faucher, Phys. Rev. A **83**, 013830 (2011).
[18] S. T. Sørensen, O. Bang, B. Wetzel, and J. M. Dudley, Opt. Commun. **285**, 2451 (2012).
[19] S. T. Sørensen, C. Larsen, U. Møller, P. M. Moselund, C. L. Thomsen, and O. Bang, J. Opt. Soc. Am. B **29**, 2875 (2012).
[20] H. G. Dantanarayana, N. Abdel-Moneim, Z. Tang, L. Sojka, S. Sujecki, D. Furniss, A. B. Seddon, I. Kubat, O. Bang, and T. M. Benson, Opt. Mater. Express **4**, 1444 (2014).
[21] M. R. Karim, B. M. A. Rahman, and G. P. Agrawal, Opt. Express **23**, 6903 (2015).